Review of downslope windstorms in Japan

Hiroyuki Kusaka[*1] and Hironori Fudeyasu[2]

[1]*Center for Computational Sciences, University of Tsukuba, 305-8577, 1-1-1 Tennodai, Tsukuba, Japan*
[2]*College of Education, Yokohama National University,
240-8501, 79-2 Tokiwadai, Hodogaya-ku, Yokohama, Japan*

Abstract. In Japan, at least 28 local winds are known by name, most of them associated with downslope windstorms and gap winds. To review these windstorms, we categorize them based largely on the atmospheric conditions and formation mechanisms, and then focus on representative examples. These representative cases include the "Yamaji-kaze", a typical downslope windstorm, the "Hirodo-kaze", a downslope windstorm induced by a nearby typhoon (intense tropical cyclone), and the "Karak-kaze", a downslope wind with a clear diurnal variation. Other downslope winds such as the "Inami-kaze" and the gap wind "Kiyokawa-dashi" are also described. Among these winds, the "Yamaji-kaze", "Hirodo-kaze", and "Kiyokawa-dashi" are considered the three most notorious due to their destructive power. After describing and comparing these winds, we discuss remaining issues to be considered in future studies.

Keywords: downslope windstorm; gap wind; local wind; Yamaji-kaze; Hirodo-kaze; Karak-kaze; Kiyokawa-dashi; numerical simulation; complex terrain

1. Introduction

A downslope windstorm blows down the lee slope of a mountain range, often reaching the foot of the mountains. The downslope windstorm has been explained as an analog to hydraulic supercritical flow (e.g., Durran and Klemp 1987, Smith 1985). Arakawa and Oobayashi (1968), as well as Houghton and Kasahara (1968), used a shallow-water-equation model with two divided layers and could simulate strong downslope wind as a hydraulic supercritical flow. Smith (1985) extended the conventional hydraulic theory to the local hydraulic theory with an atmosphere of constant stratification, and showed that mountain-wave breaking and stagnant region play important roles in forming the supercritical flow on a leeward mountain slope. Another theory of the downslope windstorm is amplification of a vertically propagating wave, with the reflection off a pre-existing or self-induced critical layer (the wave-resonance theory) (e.g., Clark and Peltier 1984, Peltier and Clark 1983). Mountain-wave breaking must be important in this theory as well as Smith's theory because it produces self-induced critical layer. Later, Durran and Klemp (1987) describe that Smith's theory may be considered as an extension of Peltier and Clark's analysis to nonlinear steady-state problems and conclude that the strong wind on a leeward mountain slope is fundamentally explained by the local hydraulic theory presuming the presence of mountain-wave

---

*Corresponding author, Professor, E-mail: kusaka@ccs.tsukuba.ac.jp

breaking.

Here, we consider the mountain and atmospheric conditions that help to create downslope windstorms. Downslope windstorms require a mountain typically range about 1-km high (or more) and a steep leeside slope (American Meteorological Society, 2016). It also helps if they have a saddle area (col) with a lower-angled slope on the upwind mountain range (e.g., Lily and Klemp 1979, Pitts and Lyons 1989, 1990, Saito 1993, Smith 1985). Favorable atmospheric conditions include an intense pressure gradient across the mountain range (moderate to strong wind component in the across-mountain-range direction) and stable stratification. An inversion layer above the mountaintop and a pre-existing critical layer are supportive conditions (e.g., Klemp and Durran 1987).

A non-dimensional mountain height $\varepsilon = NH/U$ is a widely used parameter to describe these favorable conditions. Here, N is the reference buoyancy (Brunt-Väisälä) frequency, H is the mountain ridge height, and U is a reference windspeed. As defined, ε is the inverse of the mountain Froude number. For a downslope windstorm to occur, ε should be nearly 1 or larger. For instance, Lin and Wang (1996) found that downslope windstorms occur when the mountain Froude number Fr is between 0.3 and 1.12. This condition agrees with the criteria for wave breaking, which supports the theories for downslope windstorms. More details on downslope windstorm theories are well described in Lin (2010), Markowski and Richardson (2010), and Jackson *et al*. (2012).

Downslope windstorms have been observed in many places of the world and given a variety of local names, including the "Foehn" in the foothills of the Alps (e.g., Brinkmann 1971, Jaubert and Stein 2003, Seibert 1990), the "Bora" in the Adriatic Sea (e.g., Grisogono and Belusic 2009, Lepri *et al*. 2014, Smith 1987), the "Chinook" in the foothills of the Rocky Mountains (e.g., Cook and Topil 1952, Oard 1993), the "Santa Ana" in the Los Angeles Basin (e.g., Raphael 2003, Sommers 1978), and the "Zonda" in the foothills of the Andes (e.g., Maximiliano and Nunez 2003, Norte *et al*. 2008). The "Bora" is both a cold downslope wind and a gap wind flowing between the Alps and Dinaric Alps.

For engineering applications focusing on downslope wind effects on structures and vehicles it is necessary to further elucidate characteristics of downslope windstorms in more details, as some other transient winds proved to have a strong impact on structures, e.g., Solari (2014), Aboshosha and El Damatty (2015), Solari *et al*. (2015), Yang and Zhang (2016), Lou *et al*. (2016).

Japan is a mountainous country of complex topography (Fig. 1(a)) and thus has a variety of local wind types such as the downslope windstorm and gap wind. The review here is based primarily on recent results of studies in meteorology and geography. For the relationships between these local winds, the physical geography, and the livelihoods of people, we refer readers to the earlier study of Yoshino (1975).

2. Local winds in Japan

As described in the section 1, there is a variety of local winds in Japan. Twenty-eight of these winds are mapped in Fig. 1(b). Comparison of Figs. 1(a) and 1(b) show that these local winds occur at the foot of the mountain ranges on the four big islands (Main Island, Hokkaido Island, Shikoku Island, and Kyushu Island). The names and characteristics of these winds are listed in Table 1. The names of local winds have a suffix of "kaze", "oroshi", or "dashi". The Japanese "kaze" means wind, "oroshi" means downslope windstorm or fall wind, and "dashi" suggests an
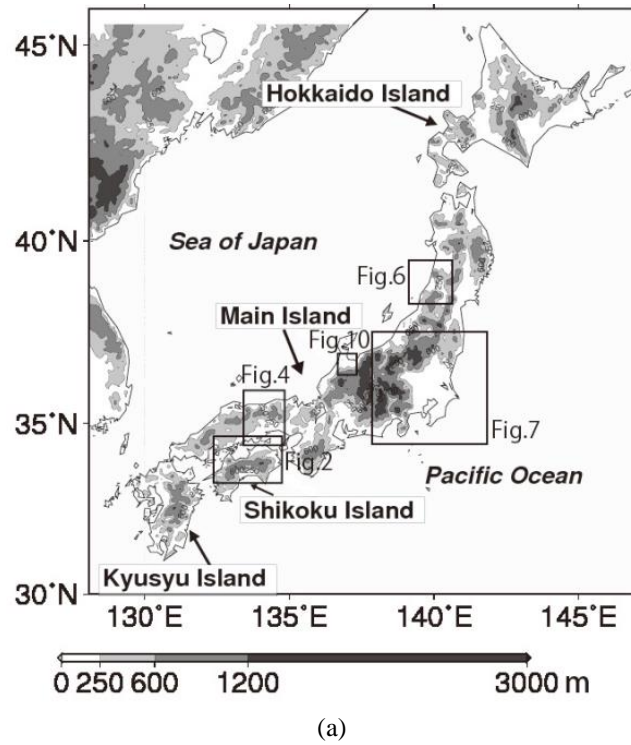
(a)

(b)

Fig. 1 (a) Topography of the four largest islands of Japan. The enlarged regional maps are in the labeled figures and (b) Distribution of local strong winds in Japan. Their name and associated weather event are listed in Table 1. (Adapted from Yoshino, 1975)

easterly wind when the boats start to sail from the shore to the sea. Most of "dashi" type is generally considered a gap wind that comes blowing from a channel between two mountain ranges or a gap in a mountain barrier (e.g., Colle and Mass 2000, Overland and Walter 1981, Reed 1931). The front part of the names comes from the local place or mountain name. These windstorms can severely damage buildings, trees, and other structures, the most notorious being the Yamaji-kaze, Hirodo-kaze, and Kiyokawa-dashi. In addition to these three, the Karak-kaze and Inami-kaze are good examples of Japanese local winds that are discussed in the present review paper.

Table 1 Name and synoptic conditions associated with local winds in Japan. The numbers refer to their location on the map in Fig. 1(b)

	Name	**Weather Chart**
1	Hikata-kaze	Cyclone
2	Tokachi-kaze	Cyclone
3	Rausu-dashi	Winter monsoon
4	Suttsu-dashi-kaze	Cyclone
5	Hidaka-shino-kaze	Toropical cyclone
6	Kiyokawa-dashi	Cyclone
7	Arakawa-dashi	Cyclone
8	Tainai-dashi	Cyclone
9	Yasuda-dashi	Cyclone
10	Nasu-oroshi	Winter monsoon
11	Akagi-oroshi	Winter monsoon
12	Haruna-oroshi	Winter monsoon
13	Tsukuba-oroshi	Winter monsoon
14	Karak-kaze	Winter monsoon
15	Dashi-no-kaze	Toropical cyclone
16	Dashi-no-kaze	Anticyclone
17	Shougawa-arashi	Anticyclone
18	Inami-kaze	Cyclone
19	Masita-kaze	Winter monsoon
20	Hira-hakko	Winter monsoon
21	Suzuka-oroshi	Winter monsoon
22	Hirano-kaze	Cyclone
23	Oroshi	Winter monsoon
24	Rokko-oroshi	Winter monsoon
25	Hirodo-kaze	Toropical cyclone
26	Yamaji-kaze	Toropical cyclone
27	Hijikawa-arashi	Anticyclone
28	Matsubori-kaze	Cyclone

3. Downslope windstorms in Japan

3.1 Yamaji-kaze

The Yamaji-kaze is a typical downslope windstorm in Japan (No. 26 in Fig. 1(b) and Table 1). It is a strong southerly wind that occurs on the northern side of the Shikoku Mountains with a mountain width of 40 km and the Niihama Plain facing the Setouchi Sea (Fig. 2). This wind had been investigated by the Japan Meteorological Agency (JMA) (e.g., Akiyama 1954, 1956). According to these studies, the Yamaji-kaze often occurs in spring and autumn, with particularly strong events happening when a well-developed extratropical cyclone passes over the Sea of Japan or a typhoon passes just west, to the northwest side of the Shikoku region. The Yamaji-kaze severely damages housings and trees. According to Yoshino (1975), wind velocities of over 15 m s^{-1} are observed 2-5 times annually. As one of the most serious disaster cases, the collapse of the steel tower (transmission line tower) in 1991 is known. On the day the tower collapsed, wind speed of 73.2 m s^{-1} was observed at the 27.5 m above ground level during the passage of Typhoon Mireille.

The Yamaji-kaze develops as follows: Before the Yamaji-kaze occurs, a northerly wind called the Sasoi-kaze (literally 'inviting wind') develops on the north side of the Shikoku Mountains. After the Sasoi-kaze blows, the southerly downslope windstorm Yamaji-kaze begins to blow in the northeast section of the Shikoku Mountains. As the Yamaji-kaze strengthens, a local front, called the "Yamaji-kaze front" forms (due to an internal hydraulic jump). The area of highest windspeed is limited to this front. Later, after the Yamaji-kaze weakens, westerly winds appear.
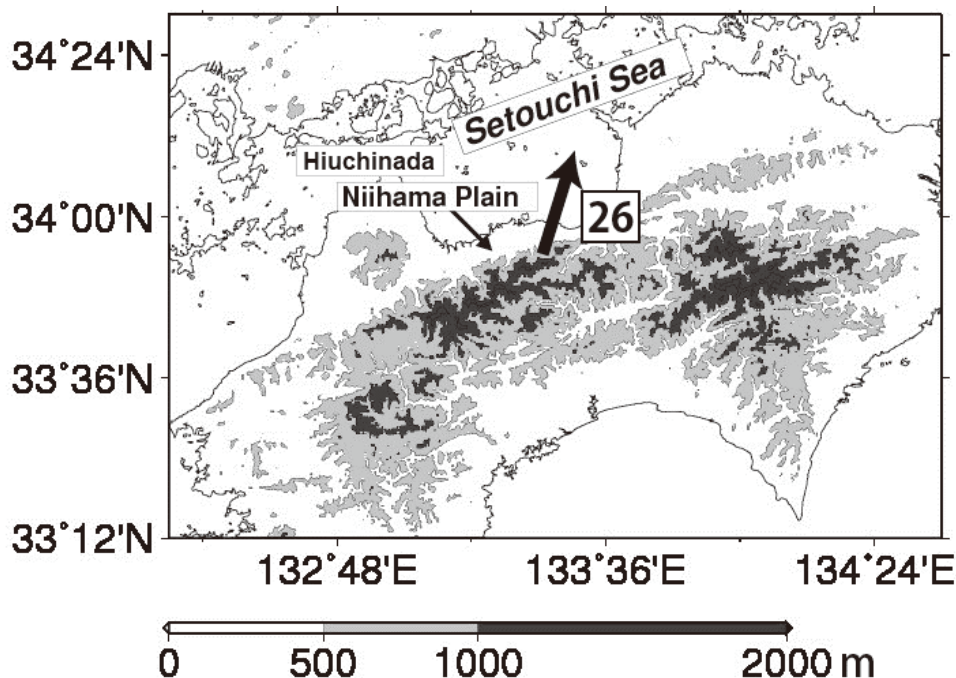

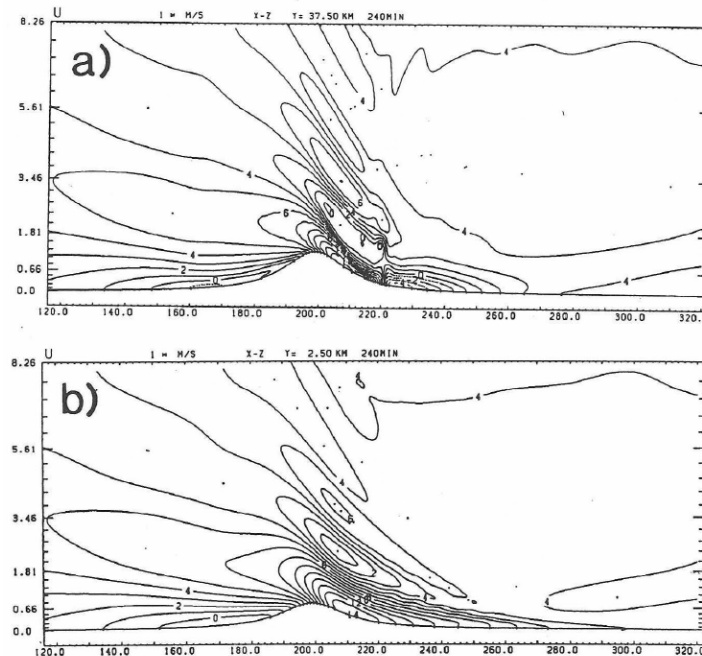Fig. 2 Topography surrounding the Yamaji-kaze area on Shikoku (see Fig. 1(a) for location)

Fig. 3 Vertical cross-section of the horizontal wind over a bell-shaped mountain range with a col. Simulated results (a) in the vicinity of the peak of the mountain and (b) in the vicinity of the col. In the diagrams, the wind is reported to blow from left to right. (Saito 1993)

A notable inversion layer is found at a level near the mountaintop for the case of the Yamaji-kaze observed on 21 April 1987. Saito and Ikawa (1991) conducted numerical experiments and confirmed that the surface wind strengthens in the presence of the inversion when compared to that without the inversion.

In a theoretical study of the Yamaji-kaze structure, Saito and Ikawa (1991) compared an analytical solution of two-dimensional flows for symmetric mountains against asymmetric mountains. The asymmetry involved mild slopes on the upwind side and steep slopes on the downwind side. They showed that asymmetric mountains tend to strengthen the mountain waves on the downwind side, with the wave-breaking occurring on the downwind slopes. Their solution supported the results from previous observational studies (e.g., Lilly and Klemp 1979, Pitts and Lyons 1989) and theoretical studies (e.g., Lily and Klemp 1979, Pitts and Lyons 1990, Smith 1985).

Saddle areas between mountain peaks, including ridgeline depressions and cols, also contribute to the formation of the Yamaji-kaze. For example, Saito (1993), in running a numerical simulation (JMA non-hydrostatic model; NHM) of the Yamaji-kaze, found that the Yamaji-kaze needs saddles (col) (Fig. 3). Moreover, the strong-wind area tends to spread forward downwind of the saddles. In this case, height of mountain and saddle area were 1050 m and 250 m, respectively. The non-dimensional mountain height ε was 2.6. Later, Saito (1994) used the same model to reproduce the Yamaji-kaze with a hydraulic jump, but was successful only when the NHM had a 2.5-km horizontal grid spacing, not a larger 10-km spacing. This series of studies confirmed that the local

characteristics of the mountain range, specifically the saddle area and mountain-slope asymmetry, have major influences on downslope windstorms. Additionally, the studies demonstrate that a numerical model with 2.5-km horizontal grid spacing is a very powerful tool for the study of downslope windstorms.

3.2 Hirodo-kaze

The Hirodo-kaze blows just south of the base of Mt. Nagi, which is located on the western main island of Japan (Fig. 4 and No. 25 in Fig. 1(b) and Table 1). It blows in an area of 10×10 km, but the most serious damages concentrated in an area of 5×2 km (Yoshino 1975). This wind mainly occurs when a typhoon approaches the region in September and October (Yoshino 1975). The Hirodo-kaze severely damages buildings, trees, and other structures. In late June 1998, for example, the Hirodo-kaze with surface wind speed over 25 m s^{-1} occurred along with Typhoon Peter and caused damages of about US $1.0 million.
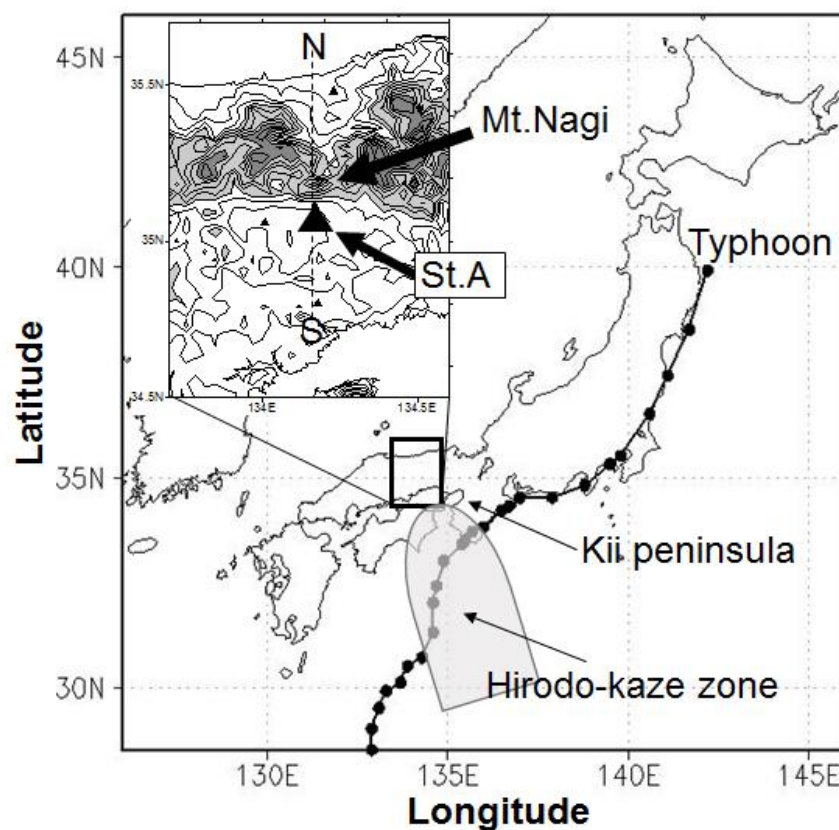

Fig. 4 Terrain around Mt. Nagi, location of the Hirodo-kaze. Contour interval is 100 m. Altitudes of 400–800 m are lightly shaded, while altitudes above 800 m are heavily shaded. Filled circles connected by a line are the locations every 3 hr of Typhoon Pabuk from JMA Best Track data. Gray zone indicates the Hirodo-kaze zone. Dashed line N–S is a cross-section used for Fig. 5
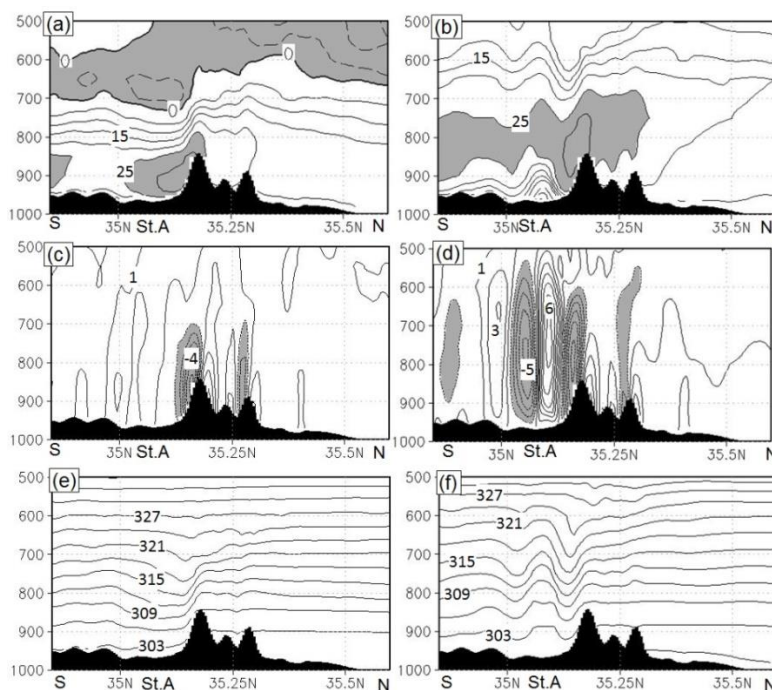
Fig. 5 Cross-section of simulated Hirodo-kaze event on 21 August 2001 at 06 UTC for the top row, 15 UTC for the bottom row. (a) and (b) are the results for meridional wind. Solid lines denote 0 m s^{-1}, broken line denotes southerlies. Contour intervals are for 5 m s^{-1}. The shaded areas indicate northerlies over 25 m s^{-1} and southerlies. (c) and (d) are the results for vertical velocity. Contour intervals are 1.0 m s^{-1}. Negative regions are shaded. (e) and (f) are the results for potential temperature. Contour intervals are 3 K. Contour longitude 134.18E. In the diagrams, the wind is reported to blow from right to left. (Fudeyasu *et al*. 2008)

Yoshino (1975) suggested that the orographic configuration of Mt. Nagi, with its steep southern slope and a mild northern slope, is favourable for downslope windstorms. Sahashi (1988), after observing a roll cloud (e.g., Vosper 2004, Vosper *et al*. 2006) parallel to the ridgeline south of Mt. Nagi during a Hirodo-kaze event, speculated that its severe winds are associated with a large-amplitude mountain wave with a rotor cloud. He also showed that the Hirodo-kaze tends to occur as a typhoon that moves northeastward over the sea southwest (offshore) of the Kii peninsula, determining a region called the "Hirodo-kaze zone" (see Fig. 4).

Fudeyasu *et al*. (2008) examined the effects of a typhoon on the occurrence of the Hirodo-kaze using the PSU/NCAR-fifth-generation Mesoscale Model (MM5) with 1-km horizontal grid spacing and 30 vertical levels. Their results, reproduced in Fig. 5, show vertical cross-sections of simulated meridional wind, vertical velocity, and potential temperature across station A at Mt. Nagi.

As the Hirodo-kaze occurred at station A, downslope windstorms developed along the lee slope of Mt. Nagi with maximum vertical velocity exceeding 6 m s^{-1} (Fig. 5(c)). Isentropes shifted downward in the lee of Mt. Nagi until they reached the lower troposphere, and they extended leeward over the base of Mt. Nagi (Fig. 5(e)), with the pre-existing critical layer near 3000 m height and the region of strong winds exceeding 25 m s^{-1} extending leeward far from Mt. Nagi (Fig.

5(a)). Strong northerlies in the lower troposphere and southerlies in the middle troposphere allowed the severe downslope windstorm to persist along the lee slope of Mt. Nagi. As the middle-tropospheric southerlies changed to northerlies, the pre-existing critical layer near 700 hPa level disappeared and the Hirodo-kaze ceased (Fig. 5(b)). Favourable atmospheric conditions for this strong-wind event arise when a typhoon passes over the sea southwest of the Kii peninsula in the Hirodo-kaze zone (see Fig. 4) and forms a pre-existing critical layer (See Fig. 5(a)).

3.3 Kiyokawa-dashi

The Kiyokawa-dashi is a strong easterly wind that blows around the Mogami Gorge in the Shonai Plain located in northern Honshu (No. 6 in Fig. 1(b)). Its strong-wind area fans out from the Gorge, but it is limited within radius of ten km (Fig. 6(a)). The Kiyokawa-dashi damages rice cultivation in this area. On the other hand, it has been also used for wind power generation.

The Kiyokawa-dashi is recognized as a gap wind, but most of the downslope winds in Japan also has features of the gap wind (Arakawa 2002) and thus it is introduced here. It occurs when an anticyclone develops over the Sea of Okhotsk or the Chishima Islands (Kuril Islands) and an extratropical cyclone moves over the Sea of Japan (Yoshino 1975).

Sasaki *et al*. (2004) investigated the vertical structure of the atmosphere during Kiyokawa-dashi events. They found that this wind occurred under a strong atmospheric stable layer (inversion layer) at a height near the mountain top. Such a stable layer is well known as a favourable atmospheric condition for gap winds. Sasaki *et al*. (2004) also found out that strong easterly winds blow at an altitude of up to 500 m, with a weaker wind above. Later, using a Coherent Doppler Lidar, Ishii *et al*. (2007) found the critical layer during a Kiyokawa-dashi event.

Recent studies have used numerical simulations to better understand the Kiyokawa-dashi. Sasaki *et al*. (2010) used the NHM to reproduce the Kiyokawa-dashi. They found good agreement with observations when the horizontal grid-spacing was respectively set to 1-km and 85 vertical levels (Fig. 6(b)). But the agreement was poor when using the model with a 5-km-horizontal grid spacing and 35 vertical atmospheric levels. The results indicated that the detailed topography of both the valley and mountains on the Kiyokawa-dashi were important.

3.4 Karak-kaze

The Karak-kaze is a dry and strong northwesterly wind frequently observed in the Kanto Plain during a typical winter monsoon (Fig. 7 and No. 14 in Fig. 1(b) and Table 1). According to Kusaka *et al*. (2011), the Karak-kaze is stronger when there is a larger northwest–southeast pressure gradient over Japan, and also when the low-pressure centre lies northwest of Hokkaido. However, the typical wind speeds of the Karak-kaze are around 10 m s^{-1} even under a large pressure gradient (Fig. 2) and lower than those of other downslope windstorms in Japan, including the Yamaji-kaze and the Hirodo-kaze. This study also showed that the Karak-kaze has a clear diurnal variation with maximum wind speed in the daytime (Fig. 8), which indicates that a significant influence on the diurnal variation is the downward momentum flux associated with a developing dry convective boundary layer. Kusaka *et al*. (2011) conducted the numerical simulations and showed that the daytime downward momentum flux and nocturnal surface inversion layer is a necessary condition for the diurnal variation of the Karak-kaze.
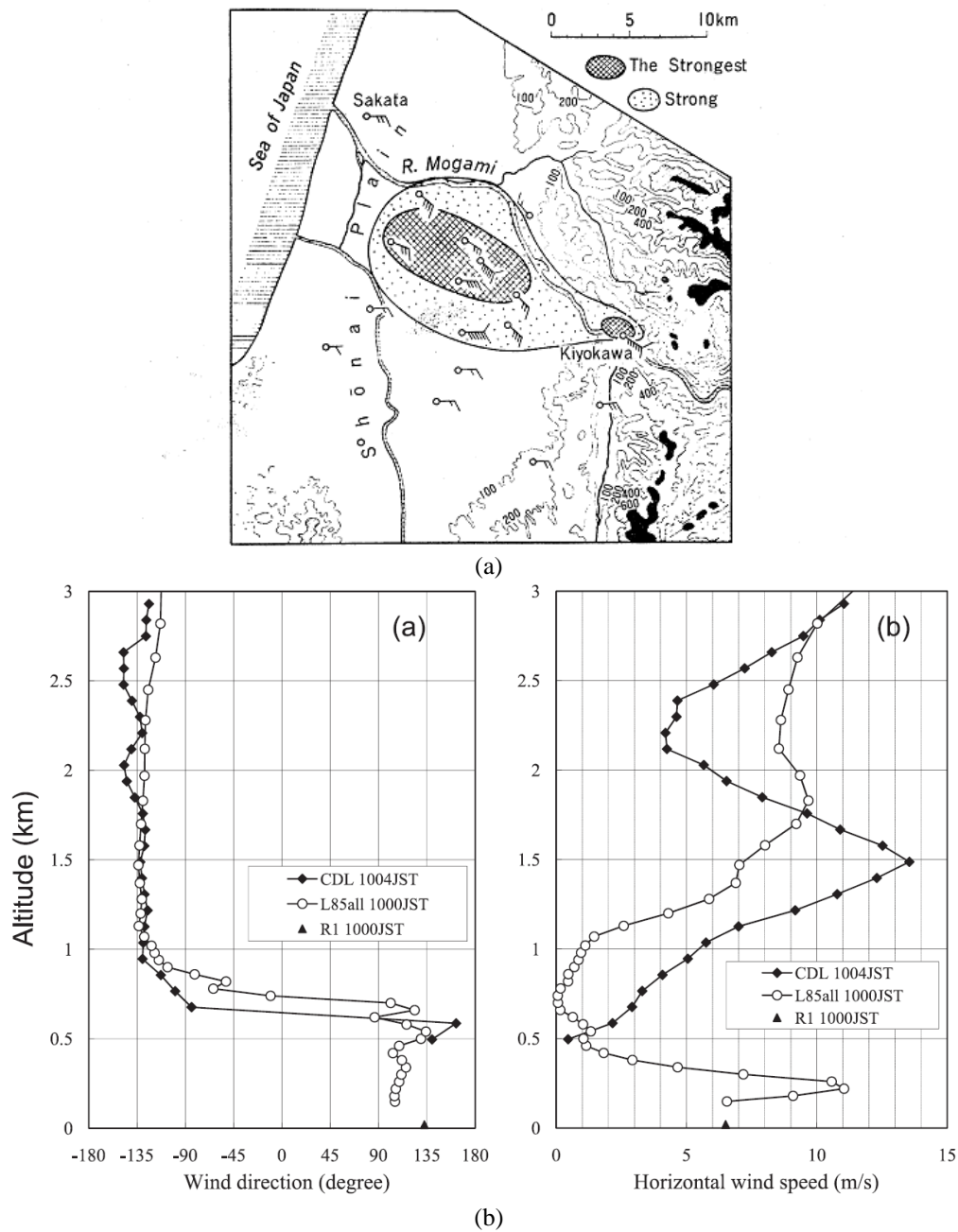
(a)

(b)

Fig. 6 (a) Horizontal distribution of surface winds during a Kiyokawa-dashi event at 10 LT 18 January 1950. (Yoshino 1975) and (b) Vertical distribution of the Kiyokawa-dashi observed by a Coherent Doppler Lidar (CDL) and simulated by the NHM with 1-km horizontal grid spacing and 85 vertical levels (L85 all). R1 indicates the observation at the surface station. Figs. 6(b) and 6(b) present wind direction and horizontal wind speed, respectively. (Sasaki *et al*. 2010)
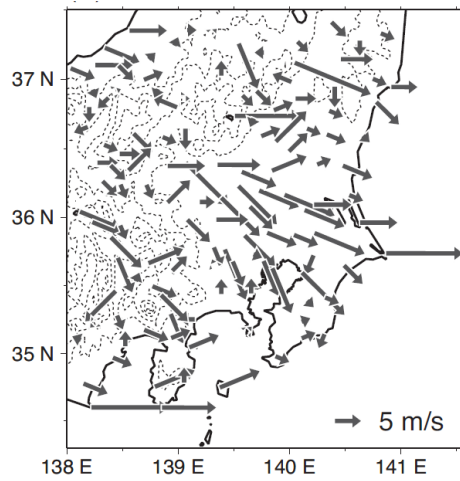
Fig. 7 Distribution of surface winds at 19 local time on February 2002 during a Karak-kaze event. Solid and broken lines indicate coastal line and terrain height, respectively. (Kusaka *et al*. 2011)
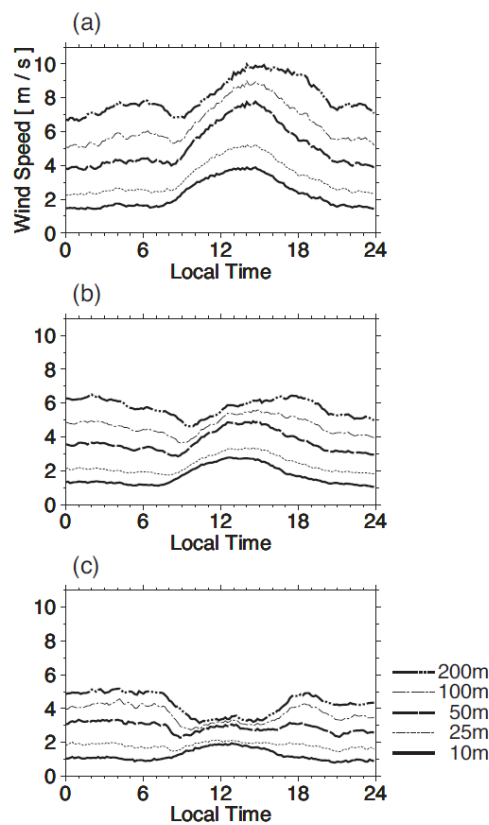

Fig. 8 Diurnal variation of wind speed from MRI tower during Karak-kaze events. (a) Average of 74 strong wind days, (b) Average of 194 medium wind days and (c) Average of 75 weak wind days. The lines indicate the observation height above ground level (Kusaka *et al*. 2011)

On the other hand, Yoshino (1975) suspected that the Karak-kaze is a kind of a Bora-type downslope windstorm from the central mountains. However, it is known that there are several types of Karak-kaze. At the moment, there is no established conceptual model of the formation mechanisms of Karak-kaze.

3.5 Foehn winds

Downslope winds can produce a large rapid temperature increase on the lee-side plain of mountains, a phenomenon well-known as a foehn. In Japan, research on foehn winds has focused on the high-temperature aspect rather than the strong winds (e.g., Arakawa *et al*. 1982, Ikawa and Nagasawa 1989, Ishizaki and Takayabu 2009, Mori and Sato 2014, Takane and Kusaka 2011, Takane *et al*. 2016). Studies revealed influences of the foehn winds on the extreme temperature events of Hokkaido Island (Mori and Sato 2014), Hokuriku region (Ishizaki and Takayabu 2009), and Kanto region (Takane and Kusaka 2011, Takane *et al*. 2016).
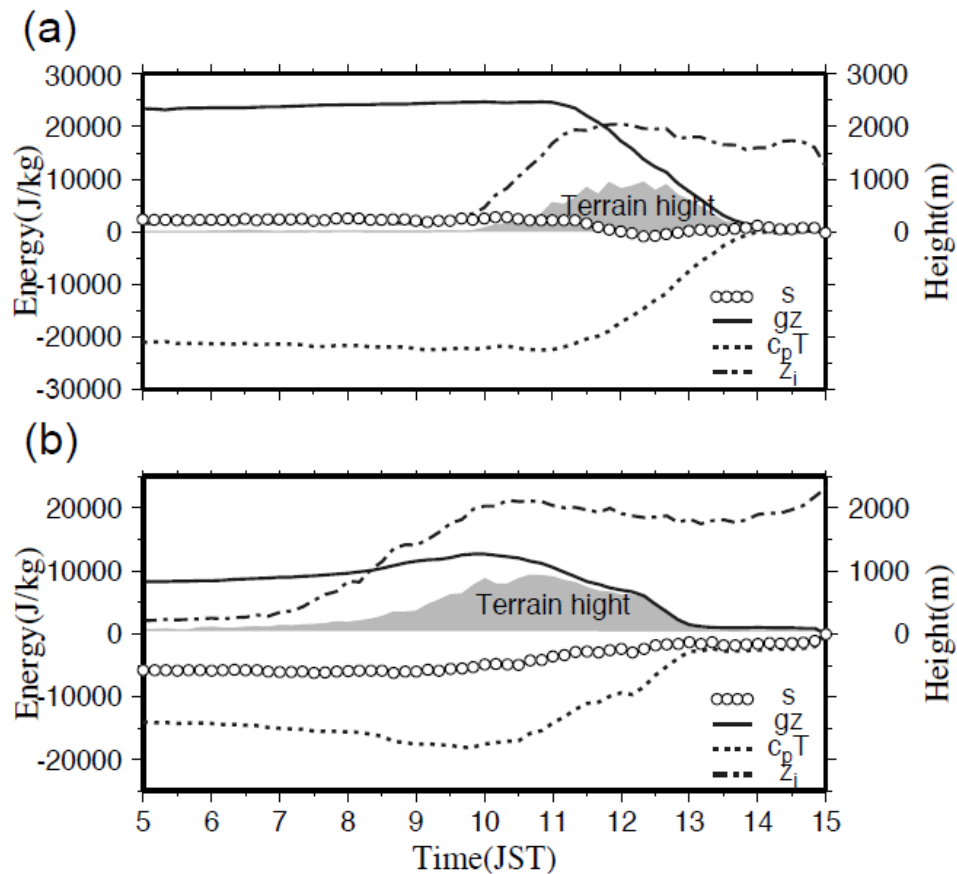

Fig. 9 The mean energy variation (J kg^{-1}) along the trajectories for course high (a) and course low (b). The solid lines indicate geopotential height gZ, dotted lines show enthalpy c_pT, the white circles show dry static energy s, and broken lines with dots show height of particle zi. Shades represent terrain height along the trajectories. (Takane and Kusaka 2011)

Downslope winds can receive some sensible heat from the leeward mountain surface. Crook and Tucker (2005) theoretically and numerically examined effects of such surface heating on airflow when it passes over such a heated mountain. Ishizaki and Takayabu (2009) showed that the dry static energy increased as airflow passed over the mountain range of mainland Japan. Later, using numerical simulations, Takane and Kusaka (2011) argued that the record-breaking extreme high temperature event of 40.9℃ observed in the inland Kanto Plain was due to foehn winds with diabatic heating from a heated mountain surface. Fig. 9 shows the Lagrangian mean energy budget along the trajectories for courses high and low. Dry static energy for course High, estimated from less particles (30% of total particles), is almost constant. On the other hand, for course Low, estimated from more particles (57% of total particles), dry static energy increases to about +5000 J kg^{-1}. This indicates the importance of diabatic heating due to surface sensible heat flux and boundary layer turbulence on the dry static energy increase, resulting in record-breaking extreme temperature. Such simulations should be tested against observations in a future study.

4. Conclusions

Numerical studies confirmed that asymmetric mountains and saddle areas (col) between mountain peaks contribute to the formation of the strong Yamaji-kaze. Additionally, it was revealed that the Hirodo-kaze occurs due to the existence of a pre-existing critical layer which forms when typhoons approach. Concerning the two most notorious downslope windstorms of Japan, the Yamaji-kaze and the Hirodo-kaze, we have a basic understanding of their essential features and formation mechanism. But for other windstorms such as the Karak-kaze, there is no established conceptual model of their formation mechanisms. In the case of some downslope windstorms such as the Inami-kaze, their small sizes (within several square kilometres), indicate that very small valleys and mountains significantly influence their formation. However, the contribution from small gaps in the mountains remains unclear. As Arakawa (2002) has pointed out, the complex topography of Japan makes it difficult to assign an individual local wind as being simply a downslope windstorm or being a gap wind. To help resolve this difficulty, numerical models with very high spatial resolution, as well as observations using remote sensing systems such as Lidar, will play important roles in explaining the mechanisms of downslope windstorms.

As spatial resolution increases, smaller-scale and steeper terrain features become more explicitly resolved. This raises challenges regarding coordinate systems and parameterization schemes when studying downslope windstorms in Japan. Many mesoscale models use a terrain-following coordinate system where only the vertical coordinate is transformed to fit the lower boundary. While this system has the advantage of having a vertical coordinate axis that uniquely determines the grid by providing topographical information, thus making it easier to describe gravity-related and boundary-layer processes, it has the disadvantage that it cannot be applied to terrain with very steep slope, for instance a slope over 45 degrees due to numerical instability and large error (Fig. 10). This is caused by the nonorthogonality of the grid system (e.g., Janjic 1989, Pielke 2001, Steppeler *et al*. 2006, Sundqvist 1976, Zängl 2003). Alternative coordinate system for the steep slope may be a generalized curvilinear coordinate system (e.g., Kajishima *et al*. 1998, Zhang *et al*. 1994) or an advanced Cartesian-grid method, for example an immersed boundary method (e.g., Fadlun *et al*. 2000, Tseng and Ferziger 2003) and a cut-cell method (a shaved-cell method) (e.g., Adcroft *et al.* 1997, Yamazaki and Satomura 2010, Ye *et al.* 1999).
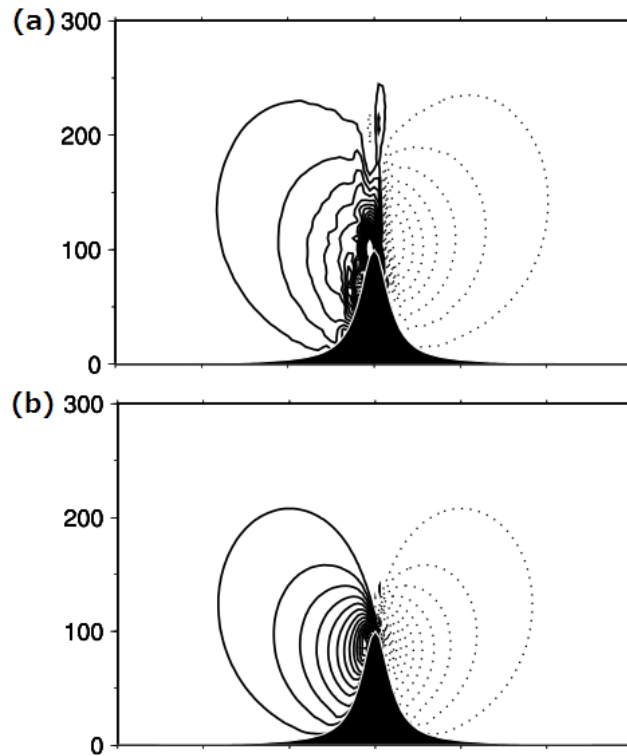
Fig. 10 Contours of vertical velocity component (interval 1 m s-1, negative values dashed) for flow over the steep slope mountain. The averaged slope angle is 59°. (a) Simulated results from the local wind model with terrain-following (z*) coordinate system and (b) simulated results from the same model but using generalized curvilinear coordinate system. In the diagrams, the wind is reported to blow from left to right. (Ikeda *et al*. 2017)

Numerical simulations of flow over mountains show that the above mentioned coordinate systems may be appropriate for simulating downslope windstorms over the steep slope (e.g., Fang and Porté-Agel 2016, Lock *et al*. 2012, Lundquist *et al*. 2010, Satomura 1989, Steppeler *et al*. 2002, Yamazaki and Satomura, 2010, 2016). A remaining issue with the use of the cut-cell method is the incorporation of physical process models and other components, such as a land-surface model because many of the physical parameterization schemes are based on a single column model (e.g., Yamazaki *et al.* 2016). The same issue remains for generalized curvilinear coordinate system. Numerical simulation of downslope windstorms is also a subject for future studies.

As the spatial resolution increases, turbulence parameterization faces challenging issues because mesoscale models traditionally use the Reynolds-Averaged Navier-Stokes (RANS) equations. Wyngaard (2004) describes that it is not clear how to apply conventional mesoscale models within the "terra incognita" region, where spatial-filter length scale (proportional to model grid interval) approaches to energy-containing turbulence scale (that may be ~100-1000 m). At this scale, it becomes theoretically inappropriate to use turbulence parameterization. Based on our experience, however, merits attained by increased resolution (by which complex terrain features are better represented in the model) well surpasses the possible downside of ignoring the

theoretical presumption for using turbulence parameterization in the "terra incognita" grey zone. Here, we will introduce a part of experimental results in our laboratory. Fig. 11 shows simulated results of a very strong downslope windstorm "Inami-kaze" (No.18 in Fig. 1(b)) from the WRF model with 300-m horizontal resolution. Using an interview survey of the local citizens, the strongest wind areas are confined to a few square kilometers, with such areas appearing several kilometres apart, generally in very small valley-like channels on the lee slope of the mountain range. Comparing the simulated results between the 50-m and 1-km mesh topography data indicates that the downslope wind blowing in a very small area requires very detailed topography data. This implies merit attended by increased resolution. However, further studies are necessary for appropriately balancing the model resolution and turbulence parameterization.

Several different types of the planetary boundary layer (PBL) schemes have been recently improved for the grey zone resolution (e.g., Ito *et al*. 2015, Kitamura 2015, Ramachandran and Wyngaard 2011, Shin and Hong 2014). Such a scheme will be adopted to community mesoscale models and used for very high resolution downslope windstorm simulations in the near future.

Large Eddy Simulation (LES) models may provide a practical approach for very high resolution simulation that can resolve energy-containing turbulence. LES model has been successfully applied to real atmospheric flow over complex terrain (e.g., Chow and Street 2009), but the applied examples are still rather sparse compared to flat terrain cases. Iizuka and Kondo (2004) investigated performance of various sub- grid scale (SGS) models in LES for atmospheric flow over idealized hills. As a result, a hybrid static/dynamic SGS model provided very accurate predictions and produced the best results of the four SGS models compared in their study. Appropriate LES model configuration for flow over complex terrain is a subject for future studies.

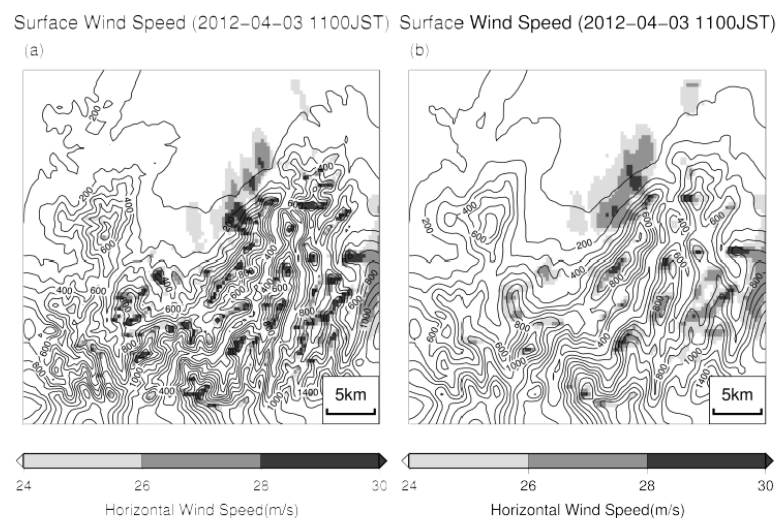Surface Wind Speed (2012-04-03 1100JST)   Surface Wind Speed (2012-04-03 1100JST)

Fig. 11 Distribution of wind speed during a simulated Inami-kaze event. Simulations performed using the WRF model with 300-m horizontal grid-spacing. Color shading and contour lines indicate the surface wind speed and terrain height, respectively. (a) 50-m resolution topography data and (b) 1-km resolution topography data. (Koyanagi and Kusaka 2017)

Coupling RANS and LES models may be still a challenging issue because LES requires boundary conditions with appropriate turbulence components and update intervals. Despite the challenge, several works have been made with the RANS and LES coupling approach (e.g., Moeng *et al*. 2007, Talbot *et al*. 2012, Wyszogrodzki *et al*. 2012). However, Michioka and Chow (2008) show that simulated results are sensitive to lateral boundary update interval. Not all studies in this field are necessarily complete.

The studies cited here have focused on dynamical processes. However, as Japan is within the Asian monsoon region, moist atmospheric physics must also be essential to understand the mechanism of downslope windstorms in Japan. Additionally, surface fluxes and boundary-layer processes play an important role of forming the Karak-kaze and Foehn winds. Thus, future studies of Japanese downslope windstorms should focus on the atmospheric physics as well as dynamics.

As it is well known, simulated results of mesoscale models are very sensitive to lateral boundary conditions (LBCs). Many of the Japanese downslope windstorms occur when a typhoon or a mid-latitude cyclone approaches. Therefore, accurate locations of typhoon or mid-latitude cyclone must be provided by LBC in order to accurately predict timing and location of downslope windstorms. In this sense, ensemble technique with different LBCs will be valuable in improving the downslope windstorm simulation.

As described earlier, pre-existing critical layer and inversion layer are often observed during the Hirodo-kaze and Kiyokawa-dashi events, which indicates importance of accurate initial conditions (ICs) resulting from data assimilation. On the other hand, Reinecke and Durran (2009) report that sensitivity to ICs is very large in the downslope wind predictions. In this sense, ensemble technique with different ICs will be appropriate.

It is considered that an ensemble prediction of wind speed using mesoscale models with different ICs/LBCs produces more spread than the models with different PBL schemes in small areas (e.g., Deppe *et al*. 2013). However, simulated results of mesoscale models depend on physics scheme selections as well. Yang *et al*. (2013) investigated the sensitivity of the WRF model's performance to the choice among three PBL schemes for simulating rapid wind speed changes (RAMP events) over a complex terrain. Their results showed that the University of Washington scheme has the best overall performance in RAMP event prediction, but no single PBL scheme is clearly superior to the others when all atmospheric conditions are considered. In this sense, PBL-scheme ensemble technique may be valuable for improving the downslope windstorm simulation as well as RAMP event simulations. Understanding the biases and strengths of mesoscale models and PBL schemes will help to improve downslope windstorm simulations.

Acknowledgments

References

Aboshosha, H. and El Damatty, A. (2015), "Dynamic response of transmission line conductors under downburst and synoptic winds", *Wind Struct.*, **21**(2), 241-272.

Adcroft, A., Hill, C. and Marshall, J. (1997), "Representation of topography by shaved cells in a height coordinate ocean model", *Mon. Weather Rev.*, **125**, 2293-2315.

Akiyama, T. (1954), "On the occurrence of the local severe wind "Yamaji". Part 1", *J. Meteorol. Res.*, (Kenkyu Jiho). **6**, 375-380. (in Japanese)

Akiyama, T. (1956), "On the occurrence of the local severe wind "Yamaji"". Part 2", *J. Meteorol. Res.*, (Kenkyu Jiho). **8**, 627-641. (in Japanese)

American Meteorological Society. (2016), Glossary of meteorology, http://glossary.ametsoc.org/wiki

Arakawa, S. (2006), "Gap wind and its brief review", *Tenki*, **53**, 161-166. (in Japanese)

Arakawa, S. and Oobayashi, T. (1968), "On the numerical experiments by the method of characteristics of one-dimensional unsteady airflow over the mountain ridge", *Papers in Meteorology and Geophysics*, **19**, 341-361.

Arakawa, S., Yamada, K. and Toya, T. (1982), "A study of foehn in the Hokuriku district using the AMeDAS data", *Papers in Meteorology and Geophysics*, **33**, 149-163.

Brinkmann, W.A.R. (1971), "What is a foehn?", *Weather*, **26**, 230-241.

Chow, F.K. and Street, R.L. (2009), "Evaluation of turbulence closure models for large-eddy simulation over complex terrain: flow over Askervein hill", *J. Appl. Meteorol. Clim.*, **48**, 1050-1063.

Clark, T.L. and Peltier, W.R. (1984), "Critical level reflection and the resonant growth of nonlinear mountain waves", *J. Atmos. Sci.*. **41**, 3122-3134.

Colle, B.A. and Mass, C.F. (2000), "High-resolution observations and numerical simulations of easterly gap flow through the strait of Juan de Fuca on 9-10 december 1995", *Mon. Weather Rev.*, **128**, 2398-2422.

Cook, A.W. and Topil, A.G. (1952), "Some examples of chinooks east of the mountains in Colorado", *Bull. Am. Meteorol. Soc.*, **33**, 42-47.

Crook, A.N. and Tucker, D.F. (2005), "Flow over heated terrain. Part I: Linear theory and idealized numerical simulations", *Mon. Weather Rev.*, **133**, 2552-2564.

Deppe, A.J., Gallus Jr. W.A. and Takle, E.S. (2013), "A WRF ensemble for improved wind speed forecasts at turbine height", *Weather Forecast.*, **28**, 212-228.

Durran, D.R. and Klemp, J. (1987), "Another look at downslope winds. Part II: Nonlinear amplification beneath wave-overturning layers", *J. Atmos. Sci.*, **44**, 3402-3412.

Fadlun, E.A., Verzicco, R., Orlandi, P. and Mohd-Yusof, J. (2000), "Combined immersed-boundary finite-difference methods for three-dimensional complex flow simulations", *J. Comput. Phys.*, **161**, 35-60.

Fang, J. And Porté-Agel, F. (2016), "Intercomparison of terrain-following coordinate transformation and immersed boundary methods for large-eddy simulation of wind fields over complex terrain", *J. Physics: Conference Series*. 753.

Fudeyasu, H., Kuwagata, T., Ohashi, Y., Suzuki, S., Kiyohara, Y. and Hozumi, Y. (2008), "Numerical study of the local downslope wind "Hirodo-kaze" in Japan", *Mon. Weather Rev.*, **136**, 27-40.

Grisogono, B. and Belušić, D. (2009), "A review of recent advances in understanding the meso- and micro-scale properties of the severe Bora wind", *Tellus*, **61**, 1-16.

Houghton, D.D. and Kasahara, A. (1968), "Non-linear shallow fluid over an isolated ridge", *Commun. Pure Appl. Math.*, **21**, 1-23.

Iizuka, S. and Kondo, H. (2004), "Performance of various sub-grid scale models in large-eddy simulation of turbulent flow over complex terrain", *Atmos. Environ.*, **38**, 7083-7091.

Ikawa, M. and Nagasawa, Y. (1989), "A numerical study of a dynamically induced foehn observed in the Abashiri-Ohmu area", *J. Meteorol. Soc. Jpn.*, **67**, 429-458.

Ikeda, R., Kusaka, H. and Iizuka, S. (2017), "Numerical simulation of flow over mountain using a local wind model with a generalized curvilinear coordinate", Private Communication.

Ishii, S., Sasaki, K., Mizutani, K., Aoki, T., Itabe, T., Kanno, H., Matsushima, D., Sha, W., Noda, A.,

Sawada, M., Ujiie, M., Matsuura, Y. and Iwasaki, T. (2007), "Temporal evolution and spatial structure of the local easterly wind "Kiyokawa-Dashi" in Japan PART I: Coherent Doppler Lidar Observations", *J. Meteorol. Soc. Jpn.*, **85**, 797-813.

Ishizaki, N. and Takayabu, I. (2009), "On the warming events over Toyama Plain by using NHRCM", *SOLA*. **5**, 129-132.

Ito, J., Niino, H., Nakanishi, M. and Moeng, C.H. (2015), "An extension of the Mellor-Yamada model to the Terra Incognita zone for dry convective mixed layers in the free convection regime", *Bound. – Lay. Meteorol.*, **157**, 23-43.

Jackson, P.L., Mayr, G. and Vosper, S. (2012), Dynamically-driven winds. p.121-218, in "Mountain Weather Research and Forecasting", (Eds., Chow, F.K., De Wekker, S.F.J., Snyder, B.J.), Springer.

Janjić, Z.I. (1989), "On the pressure gradient force error in s-coordinate spectral models", *Mon. Weather Rev.*, **117**, 2285-2292.

Jaubert, G. and Stein, J. (2003), "Multiscale and unsteady aspects of a deep föhn event during MAP", *Q. J. Roy. Meteorol. Soc.*, **129**, 755-559.

Kajishima, T., Ohta, T., Okazaki, K. and Miyake, Y. (1998), "High-order finite-difference method for incompressible flows using collocated grid system", *JSME International, Ser. B.*, **41**, 830-839.

Kitamura, Y. (2015), "Estimating dependence of the turbulent length scales on model resolution based on a priori analysis", *J. Atmos. Sci.*, **72**, 750-762.

Klemp, J.B. and Durran, D.R. (1987), "Numerical modeling of bora winds", *Meteorol. Atmos. Phys.*, **36**, 215-227.

Koyanagi, T. and Kusaka, H. (2017), "Numerical simulation of the downslope windstorm "Inami-kaze" in Tonami plain using the WRF model with 50-m and 1-km resolution terrain data", Private Communication.

Kusaka, H., Miya, Y. and Ikeda, R. (2011), "Effects of solar radiation amount and synoptic-scale wind on the local wind "Karakkaze" over the Kanto plain in Japan", *J. Meteorol. Soc. Jpn*, **89**, 327-340.

Lepri, P., Kozmar, H., Večenaj, Ž. and Grisogono, B. (2014), "A summertime near-ground velocity profile of the Bora wind", *Wind Struct.*, **19**(5), 505-522.

Lilly, D.K. and Klemp, J.B. (1979), "The effect of terrain shape on non-linear hydrostatic mountain waves", *J. Fluid Mech.*, **95**, 241-261.

Lin, Y.L. (2010), "Mesoscale Dynamics", Cambridge University Press, pp. 630.

Lin, Y.L. and Wang, T.A. (1996), "Flow regimes and transient dynamics of two-dimensional stratified flow over an isolated mountain ridge", *J. Atmos. Sci.*, **53**, 139-158.

Lock, S.J., Bitzer, H.W., Coals, A., Gadian, A. and Mobbs, S. (2012), "Demonstration of a cut-cell representation of 3D orography for studies of atmospheric flows over very steep hills", *Mon. Weather Rev.*, **140**, 411-424.

Lou, W.J., Wang, J.W., Chen, Y., Lv, Z.B. and Lu, M. (2016), "Effect of motion path of downburst on wind-induced conductor swing in transmission line", *Wind Struct.*, **23**(3), 41-59.

Lundquist, K.A., Chow, F.K. and Lundquist, J.K. (2010), "An immersed boundary method for the weather research and forecasting model", *Mon. Weather Rev.*, **138**, 796-817.

Markowski, P. and Richardson, Y. (2010), "Mesoscale Meteorology in Midlatitudes" Wiley-Blackwell, 407.

Maximiliano, V.M. and Nunez, N. (2003), "Analysis of three situations of the Foehn effect over the Andes (zonda wind) using the Eta-CPTEC regional model", *Weather Forecast.*, **18**, 481-501.

Michioka, T. and Chow, F.K. (2008), "High-resolution large-eddy simulations of scalar transport in atmospheric boundary layer flow over complex terrain", *J. Appl. Meteorol. Clim.*, **47**, 3150-3169.

Moeng, C.H., Dudhia, J., Klemp, J. and Sullivan, P. (2007), "Examining two-way grid nesting for large eddy simulation of the PBL using the WRF model", *Mon. Weather Rev.*, **135**, 2295-2311.

Mori, K. and Sato, T. (2014), "Spatio-temporal variation of high-temperature events in Hokkaido, North Japan", *J. Meteorol. Soc. Jpn*, **92**, 327-346.

Norte, F.A., Ulke, A.G., Simonelli, S.C. and Viale, M. (2008), "The severe zonda wind event of 11 July 2006 east of the Andes Cordillera (Argentine): a case study using the BRAMS model", *Meteorol. Atmos. Phys.*, **102**, 1-14.

Oard, M.J. (1993), "A method for predicting Chinook winds east of the Montana Rockies", *Weather*

Forecast., **8**, 166-180.

Overland, J.E. and Walter, B.A. (1981), "Gap winds in the Strait of Juan de Fuca", *Mon. Weather Rev.*, **109**, 2221-2233.

Peltier, W.R. and Clark, T.L. (1983), "Nonlinear mountain waves in two and three spatial dimensions", *Q. J. Roy. Meteorol. Soc.*, **109**, 527-548.

Pielke, R.A. (2001), "Mesoscale Meteorological Modeling", 2nd Ed., Academic Press.

Pitts, R.O. and Lyons, T.J. (1989), "Airflow over a two-dimensional escarpment. I: Observations", *Q. J. Roy. Meteorol. Soc.*, **115**, 965-981.

Pitts, R.O. and Lyons, T.J. (1990), "Airflow over a two-dimensional escarpment. II: Hydrostatic flow", *Q. J. Roy. Meteorol. Soc.*, **116**, 363-378.

Ramachandran, S. and Wyngaard, J.C. (2011), "Subfilter-scale modelling using transport equations: large-eddy simulation of the moderately convective atmospheric boundary layer", *Bound. – Lay. Meteorol.*, **139**, 1-35.

Raphael, M.N. (2003), "The Santa Ana winds of California", *Earth Interactions*, **7**, 1-13.

Reed, T.R. (1931), "Gap winds of the Strait of Juan de Fuca", *Mont. Weather Rev.*, **59**, 373-376.

Reinecke, P.A. and Durran, D.R. (2009), "Initial condition sensitivities and the predictability of downslope winds", *J. Atmos. Sci.*, **66**, 3401-3418.

Sahashi, K. (1988), "A roll accompanied by HIROTO-KAZE", *Tenki*, **35**, 497-499. (in Japanese)

Saito, K. (1993), "A numerical study of the local downslope wind "Yamaji -kaze" in Japan. Part 2: Non-linear aspect of the 3-D flow over a mountain range with a col.", *J. Meteorol. Soc. Jpn*, **71**, 247-271.

Saito, K. (1994), "A numerical study of the local downslope wind "Yamaji-kaze" in Japan. Part 3: Numerical simulation of the 27 September 1991 windstorm with a nonhydrostatic multi-nested model", *J. Meteorol. Soc. Jpn*, **72**, 301-329.

Saito, K. and Ikawa, M. (1991), "A numerical study of the local downslope wind "Yamaji-kaze" in Japan", *J. Meteorol. Soc. Jpn*, **69**, 31-56.

Sasaki, K., Kanno, H., Yokoyama, K., Matsushima, D., Moriyama, M., Fukabori, K. And Sha, W. (2004), "Observational evidence of the spatial distribution of wind speed and the vertical structure of the local easterly strong wind "Kiyokawa-dashi" on the Shonai Plain, Yamagata", *Tenki*, **51**, 881-894. (in Japanese)

Sasaki, K., Sawada, M., Ishiim, S., Kanno, H., Mizutani, K., Aoki, T., Itabe, T., Matsushima, D., Sha, W., Noda, A.T., Ujiie, M., Matsuura, Y. and Iwasaki, T. (2010), "The temporal evolution and spatial structure of the local easterly wind "Kiyokawa-dashi" in Japan. Part II: Numerical simulations", *J. Meteorol. Soc. Jpn*, **88**, 161-181.

Satomura, T. (1989), "Compressible flow simulations on numerically generated grids", *J. Meteorol. Soc. Jpn*, **67**, 473-482.

Seibert, P. (1990), "South foehn studies since the ALPEX experiment", *Meteorol. Atmos. Phys.*, **43**, 91-103.

Shin, H.H. and Hong, S.Y. (2014), "Representation of the subgrid-scale turbulent transport in convective boundary layers at gray-zone resolutions", *Mon. Weather Rev.*, **143**, 250-271.

Smith, R.B. (1985), "On severe downslope winds", *J. Atmos. Sci.*, **42**, 2597-2603.

Smith, R.B. (1987), "Aerial observations of the Yugoslavian bora", *J. Atmos. Sci.*, **44**, 269-297.

Solari, G. (2014), "Emerging issues and new frameworks for wind loading on structures in mixed climates", *Wind Struct.*, **19**(3), 295-320.

Solari, G., Burlando, M., De Gaetano, P. and Repetto, M.P. (2015), "Characteristics of thunderstorms relevant to the wind loading of structures", *Wind Struct.*, **20**(6), 763-791.

Sommers, W.T. (1978), "LFM forecast variables related to Santa Ana wind occurrences", *Mon. Weather Rev.*, **106**, 1307-1316.

Steppeler, J., Bitzer, H. W., Janjic, Z., Schättler, U., Prohl, P., Gjertsen, U., Torrisi, L., Parfinievicz, J., Avgoustoglou, E. and Damrath, U. (2006), "Prediction of clouds and rain using a z-coordinate nonhydrostatic model", *Mon. Weather Rev.*, **134**, 3625-3643.

Steppeler, J., Bitzer, H.W., Minotte, M. and Bonaventura, L. (2002), "Nonhydrostatic atmospheric modeling using a z-coordinate representation", *Mon. Weather Rev.*, **130**, 2143-2149.

Sundqvist, H. (1976), "On vertical interpolation and truncation in connection with use of sigma system

models", *Atmosphere*, **14**, 37-52.

Takane, Y. and Kusaka, H. (2011), "Formation mechanisms of the extreme high surface air temperature of 40.9°C observed in the Tokyo metropolitan area: Considerations of dynamic foehn and foehn like wind", *J. Appl. Meteorol. Clim.*, **50**, 1827-1841.

Takane, Y., Kusaka, H. and Kondo, H. (2016), "Investigation of a recent extreme high-temperature event in the Tokyo metropolitan area using numerical simulations: the potential role of a 'hybrid' foehn wind", *Q. J. Roy. Meteorol. Soc.*, **141**, 1857-1869.

Talbot, C., Bou-Zeid, E. and Smith, J. (2012), "Nested mesoscale large-eddy simulations with WRF: Performance in real test cases", *J. Hydrometeorol.*, **13**, 1421-1441.

Tseng, Y.H. and Ferziger, J.H. (2003), "A ghost-cell immersed boundary method for flow in complex geometry", *J. Comput. Phys.*, **192**, 593-623.

Vosper, S.B. (2004), "Inversion effects on mountain lee waves", *Q. J. Roy. Meteorol. Soc.*, **130**, 1723-1748.

Vosper, S.B., Sheridan, P.F. and Brown A.R. (2006), "Flow separation and rotor formation beneath two-dimensional trapped lee waves", *Q. J. Roy. Meteorol. Soc.*, **132**, 2415-2438.

Wyngaard, J.C. (2004), "Toward numerical modeling in the "Terra Incognita", *J. Atmos. Sci.*, **61**, 1816-1826.

Wyszogrodzki, A.A., Miao, S. and Chen, F. (2012), "Evaluation of the coupling between mesoscale-WRF and LES-EULAG models for simulating fine-scale urban dispersion", *Atmos. Res.*, **118**, 324-345.

Yamazaki, H. and Satomura, T. (2010), "Nonhydrostatic atmospheric modeling using a combined Cartesian grid", *Mon. Weather Rev.*, **138**, 3932-3945.

Yamazaki, H., Satomura, T. and Nikiforakis, N. (2016), "Three-dimensional cut-cell modelling for high-resolution atmospheric simulations", *Q. J. Roy. Meteorol. Soc.*, **142**, 1335-1350.

Yang, F.L. and Zhang, H.J. (2016), "Two case studies on structural analysis of transmission towers under downburst", *Wind Struct.*, **22**(6), 685-701.

Yang, Q.L., Berg, L.K., Pekour, M., Fast, J.D. and Newson, R.N. (2013), "Evaluation of WRF-predicted near-hub-height winds and ramp events over a Pacific northwest site with complex terrain", *J. Appl. Meteorol. Clim.*, **52**, 1753-1763.

Ye, T., Mittal, R., Udaykumar, H.S. and Shyy, W. (1999), "An accurate Cartesian grid method for viscous incompressible flows with complex immersed boundaries", *J. Comput. Phys.*, **156**, 209-240.

Yoshino, M. (1975), "Climate in a small area", 549, University of Tokyo Press, Tokyo, Japan.

Zang, Y., Street, R.L. and Koseff, J.R. (1994), "A non-staggered grid, fractional step method for time-dependent incompressible Navier-Stokes equation in curvilinear coordinates", *J. Comput. Phys.*, **114**, 18-33.

Zängl, G. (2003), "A generalized sigma-coordinate system for the MM5", *Mon. Weather Revi.*, **131**, 2875-2884.